

1
2
3
4
5
6
7
8
9
10
11
12
13
14
15
16
17
18
19
20
21
22
23
24

Depth profiling of carbon and nitrogen in copper using nuclear reactions

T. Thomé, J. L. Colaoux and G. Terwagne

Laboratoire d'Analyses par Réactions Nucléaires, Facultés Universitaires Notre-Dame de la Paix, B-5000 Namur, Belgium

Abstract

Simultaneous implantations of ^{12}C and ^{15}N were performed into copper using the non deviated beam line of a 2 MV Tandetron accelerator. The atomic composition of the implanted layer was measured using appropriate nuclear reactions with a 1.05 MeV deuteron beam. $^{12}\text{C}(\text{d},\text{p}_0)^{13}\text{C}$ and $^{15}\text{N}(\text{d},\alpha_0)^{13}\text{C}$ nuclear reactions were used to depth profile simultaneously ^{12}C and ^{15}N and to determine the relative contribution of multi-ionised ^{12}C and ^{15}N ions to the carbon and nitrogen distribution. We also used the narrow resonance at 429 keV of the $^{15}\text{N}(\text{p},\alpha\gamma)^{12}\text{C}$ nuclear reaction to check the validity of our results . The depth distributions obtained with this resonant nuclear reaction confirmed that (d,p) and (d, α) reactions are well suited to profile both carbon and nitrogen elements with a quite good resolution. Moreover, using these reactions makes possible to profile ^{12}C and ^{15}N atoms with a single and relatively rapid measurement.

PACS codes : 25.40.Ny, 25.45.De, 29.30.Ep

Keywords : depth profiling, ^{15}N , NRA, RNRA, $^{15}\text{N}(\text{d},\alpha_0)^{13}\text{C}$, $^{15}\text{N}(\text{p},\alpha\gamma)^{12}\text{C}$

Corresponding author : T. Thomé, FUNDP, 61 rue de Bruxelles, B-5000 Namur, Belgium

E-mail : tristan.thome@fundp.ac.be - Phone : 32 (0) 81 72 54 77

25 **1. Introduction**

26 In recent years, the synthesis of crystalline carbon nitride C_3N_4 has been extensively
27 investigated due to its highly interesting mechanical properties. Indeed, some calculations
28 predicted that several structures as β - C_3N_4 would be harder than diamond [1]. So far,
29 whatever the technique employed, mixed phase layers are quite often obtained and it remains
30 very difficult to achieve fully crystalline phase formation [2-4]. Among these techniques, ion
31 implantation may be an interesting solution, even if successive carbon and nitrogen
32 implantations in metals have not yet been conclusive [5].

33 In this work, we performed different types of implantations with carbon ^{12}C and
34 nitrogen ^{15}N ions into copper samples. Then, we determined the depth distributions of ^{12}C and
35 ^{15}N using $^{12}C(d,p_0)^{13}C$ and $^{15}N(d,\alpha_0)^{13}C$ nuclear reactions with a 1.05 MeV deuteron beam.
36 We also compared the ^{15}N implantation depth profiles determined by this NRA method with
37 the ones obtained using the resonant $^{15}N(p,\alpha\gamma)^{12}C$ nuclear reaction [6].

38

39 **2. Experimental**

40 The samples were polished polycrystalline copper substrates. Two types of
41 implantations were carried out with our 2 MV Tandetron accelerator (ALTAÏS¹); a successive
42 nitrogen $^{15}N^+$ and $^{15}N^{2+}$ implantation on a deflected beam line (first implantation), and a
43 simultaneous multi-ionised ^{12}C and ^{15}N implantation on a non deflected beam line (second
44 implantation). To perform these implantations, CN^- anions were produced by a Cs sputter ion
45 source and injected in the low energy part of the Tandetron accelerator. After passing through
46 the gas exchange channel, a large variety of C^{n+} and N^{q+} ions were produced leading to
47 different energies for carbon and nitrogen ions (Table1) in the non deviated beam line. During
48 both implantations, the samples were maintained at room temperature and the vacuum

¹ Accélérateur Linéaire Tandetron pour l'Analyse et l'Implantation des Solides

49 pressure did not exceed 10^{-5} Pa. The terminal voltage of the accelerator was fixed at 400 kV
50 for all the implantations. In the first implantation, the nitrogen $^{15}\text{N}^{2+}$ was implanted in first
51 place. The corresponding energy was 1050 keV with a current density of $3\ \mu\text{A}\cdot\text{cm}^{-2}$ and the
52 final dose was $10^{17}\ \text{at}\cdot\text{cm}^{-2}$ over a $5\times 5\ \text{mm}^2$ area. The nitrogen $^{15}\text{N}^+$ implantation was
53 performed on the same target spot with an energy of 648 keV and a current density of
54 $6\ \mu\text{A}\cdot\text{cm}^{-2}$. The final dose was $2\times 10^{17}\ \text{at}\cdot\text{cm}^{-2}$. The energies of $^{15}\text{N}^+$ and $^{15}\text{N}^{2+}$ ions
55 corresponded to implantation projected ranges respectively close to 580 and 820 nm in
56 copper, according to SRIM2003 code calculations (Table 1) [7]. During the second
57 implantation performed on the non deviated beam line of the accelerator, the current density
58 was measured around $20\ \mu\text{A}\cdot\text{cm}^{-2}$ and the total final dose (including C and N ions) was
59 estimated at $10^{18}\ \text{at}\cdot\text{cm}^{-2}$.

60 The depth distribution of nitrogen ^{15}N in the first implantation and the ones of carbon
61 ^{12}C and nitrogen ^{15}N in the second implantation were determined with resonant (RNRA) and
62 non resonant (NRA) nuclear reactions using the same facilities as for the implantations. For
63 NRA analyses, ^{15}N and ^{12}C atoms were depth profiled using $^{15}\text{N}(\text{d},\alpha_0)^{13}\text{C}$ and $^{12}\text{C}(\text{d},\text{p}_0)^{13}\text{C}$
64 nuclear reactions with a 1.05 MeV deuteron beam. Two silicon surface barrier detectors were
65 fixed at 150° and 165° relative to the incident beam to measure respectively NRA and RBS
66 signals. A $12\ \mu\text{m}$ mylar absorber foil was placed in front of the NRA detector (25.7 msr) to
67 stop backscattered ions and to measure energetic α and proton particles. The RBS detector
68 was collimated (0.18 msr) to allow the detection of backscattered deuterons without any
69 absorber foil. The RBS detector was used as a monitor to determine the quantity of incident
70 deuterons during the measurements. For RNRA analyses, we considered the very narrow
71 resonance at 429 keV (width of 120 eV) of the $^{15}\text{N}(\text{p},\alpha\gamma)^{12}\text{C}$ nuclear reaction [6]. A NaI
72 scintillation detector was used to detect the gamma radiation emitted at 4.43 MeV by the
73 nuclear reaction. The ^{15}N depth profiling was carried out by varying the energy of the incident

74 proton beam from 420 to 700 keV with 2 keV steps. A chromium nitride sample with a well
75 defined atomic composition was used as a reference for the determination of absolute
76 concentrations.

77

78 **3. Results and discussion**

79 Fig. 1a and 1b show the experimental NRA spectra measured at 150° for the first and
80 the second implantation. A very intense peak is observed in both spectra just below 3 MeV,
81 which can be attributed to ^{12}C surface contamination in the first implantation and to a mixing
82 between surface contamination and implanted ^{12}C ions in the second one. The peak detected
83 around 4 MeV corresponds to the (d, α) reaction with the implanted ^{15}N ions. Another peak
84 below 6 MeV is assigned to the (d,p) reaction with ^{13}C isotopes. We can observe that all the
85 peaks are broader for the second implantation where multi-ionised ions with different energies
86 are implanted (Table 1). From these spectra, we determined the total concentrations and the
87 depth distributions of ^{12}C and ^{15}N elements using the SIMNRA program [8]. The simulated
88 SIMNRA spectra are presented in Fig. 1 and the different calculated depth profiles of ^{12}C and
89 ^{15}N are shown in Fig. 2 and Fig. 3.

90 In the first implantation, the total nitrogen concentration calculated from the curve area
91 in Fig. 2a ($2.5 \times 10^{17} \text{ at.cm}^{-2}$) corresponds well to the expected one. The corresponding ^{12}C
92 depth distribution is not reported here as ^{12}C presence is mainly due to a 50 nm thick surface
93 contamination layer occurring during ion implantation (carbon build-up phenomenon [9]).
94 The experimental distribution maxima, respectively close to 600 and 860 nm for $^{15}\text{N}^+$ and
95 $^{15}\text{N}^{2+}$ ions, correspond well with the projected ranges calculated with SRIM2003 program
96 (Table 1). In the second implantation, several distributions are observed around a main peak
97 which corresponds to $^{15}\text{N}^+$ implanted ions. From the comparison with the distribution
98 obtained in the first implantation and from the SRIM2003 calculated projected ranges

99 (table 1), we can attribute the first shoulder around 300 nm to neutral ^{15}N implanted atoms
100 and the 3 other ones at 880, 1020 and 1200 nm to respectively $^{15}\text{N}^{2+}$, $^{15}\text{N}^{3+}$, and $^{15}\text{N}^{4+}$
101 implanted ions. A ^{15}N surface peak is also detected, which can be explained by a diffusion
102 process of nitrogen during the implantation.

103 Then, we used the resonance at 429 keV of the $^{15}\text{N}(p,\alpha\gamma)^{12}\text{C}$ nuclear reaction to confirm
104 the validity of the results obtained by NRA for both implantations. The ^{15}N depth
105 distributions obtained by RNRA are shown in Fig.2. The NRA ^{15}N depth profiles are
106 relatively close to the RNRA ones, and the contributions of different multi-ionised carbon and
107 nitrogen ions are clearly revealed by both techniques. Although we have not estimated the
108 exact depth resolution of the NRA method used in our experiments, the RNRA results
109 confirm that (d, α) nuclear reactions are well suited to profile nitrogen elements with a quite
110 good resolution. In Fig. 3 are shown the depth profiles of nitrogen and carbon ions determined
111 by the NRA method for the second implantation. A very thin ^{12}C contamination layer
112 (< 2 nm), characteristic of the carbon build-up phenomenon, is detected [9]. This carbon layer
113 is not visible in the Fig. 3 due to too small scales. As for the ^{15}N depth profile, a shoulder
114 attributed to neutral ^{12}C implanted species, is detected before the main peak (corresponding to
115 $^{12}\text{C}^+$ ions), but only one is observed for deeper ranges. It indicates that only very small
116 quantities of $^{12}\text{C}^{3+}$ and $^{12}\text{C}^{4+}$ ions are present in the implantation ion beam. This was
117 confirmed measuring the different intensities of multi-ionised carbon ion beam on a deviated
118 beam line of the accelerator. We can also remark that the nitrogen and carbon total
119 concentrations simultaneously implanted on the non deviated line are quite equal, which is
120 interesting for the purpose of forming carbon nitride compounds close to the C_3N_4
121 stoichiometry.

122

123 **4. Conclusion**

124 We showed that $^{12}\text{C}(\text{d},\text{p}_0)^{13}\text{C}$ and $^{15}\text{N}(\text{d},\alpha_0)^{13}\text{C}$ nuclear reactions are well suited to
125 profile both carbon and nitrogen elements in a single and relatively rapid measurement and
126 with a quite good resolution. After a simultaneous carbon and nitrogen implantation, we were
127 able to distinguish the relative contributions of multi-ionised elements to the total depth
128 profiles. Moreover, the distributions of nitrogen ^{15}N obtained by RNRA, using the
129 $^{15}\text{N}(\text{p},\alpha\gamma)^{12}\text{C}$ reaction, were very close to the ones determined by NRA. The strong correlation
130 in shape and in concentration between the ^{15}N and ^{12}C depth profiles suggests that carbon
131 nitrides close to the C_3N_4 stoichiometry may be synthesized in copper.

132

133 **References**

- 134 [1] A. Lui, M. Cohen, *Science* **247** (1989) 688
- 135 [2] C. Niu, Y.Z. Lu, C.M. Lieber, *Science* **261** (1993) 334
- 136 [3] A. Hoffman, I. Gouzman and R. Brener, *Appl. Phys. Lett.* **64** (1994) 845
- 137 [4] N. Hellgren, M.P. Johansson, E. Broitman, L. Hultman and J.-E. Sundgren, *Phys. Rev. B*
138 **59** (1999) 5162
- 139 [5] R. Sanchez, J. A. Garcia, A. Medrano, M. Rico, R. Martinez, R. Rodriguez, C. Fernandez-
140 Ramos, A. Fernandez, *Surface and Coatings Technology* **158-159** (2002) 630
- 141 [6] B. Maurel and G. Amsel, *Nucl. Instr. Meth. B* **218** (1983) 159
- 142 [7] J.F. Ziegler, J.P. Biersack, U. Littmark, *The Stopping and Range of Ions in Solids*,
143 Pergamon, New York, 1967
- 144 [8] M. Mayer, SIMNRA, Proc. 15th Int. Conf. Appl. Accelerators in Research and Industry, J.
145 L. Duggan and I. L. Morgan (eds.), *AIP Conf. Proc.* **475** (1999) 541
- 146 [9] J. Colaux, G. Terwagne, *Nucl. Instr. Meth. B* **240** (2005) 429

147

148 **Tables**

149

150 Table 1: Energies of implantation and experimental (R_{exp}) and calculated (R_{SRIM}) projected
 151 ranges of ^{12}C and ^{15}N ion depth distributions in copper for a terminal voltage of
 152 400 kV on our Tandetron accelerator.

153

	E (keV)	R_{SRIM} (nm)	R_{exp} (nm) 1 st implantation	R_{exp} (nm) 2 nd implantation
C	195	240	-	300
C ⁺	600	585	-	600
C ²⁺	1000	840	-	880
N	243	250	-	300
N ⁺	648	580	600	600
N ²⁺	1050	820	860	880
N ³⁺	1450	1000	-	1020
N ⁴⁺	1860	1180	-	1200

154

155

156 **Figure captions**

157

158 Figure 1: Experimental (dots) and simulated (solid lines) NRA spectra at 150° of the copper
159 sample implanted at room temperature with (a) $^{15}\text{N}^+$ and $^{15}\text{N}^{2+}$ (1st implantation) and
160 (b) $^{12}\text{C}^{n+}$ and $^{15}\text{N}^{p+}$ (2nd implantation on the non deviated beam line).

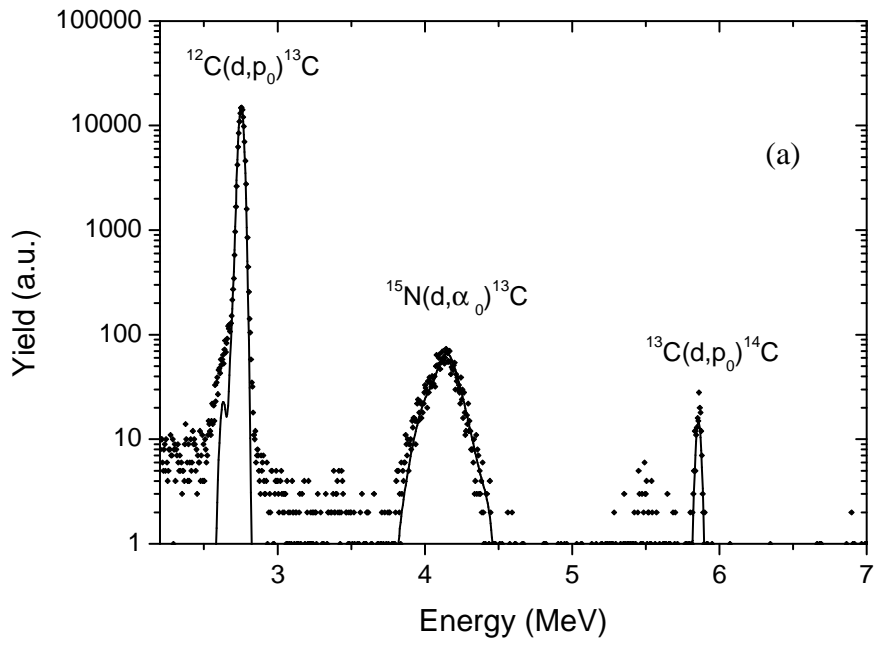
161

162 Figure 2: Depth distributions of ^{15}N ions determined from SIMNRA simulations (open
163 squares) and from RNRA measurements (solid lines) for the copper samples
164 implanted with (a) $^{15}\text{N}^+$ and $^{15}\text{N}^{2+}$ (1st implantation) and (b) $^{12}\text{C}^{n+}$ and $^{15}\text{N}^{p+}$ (2nd
165 implantation on the non deviated beam line).

166

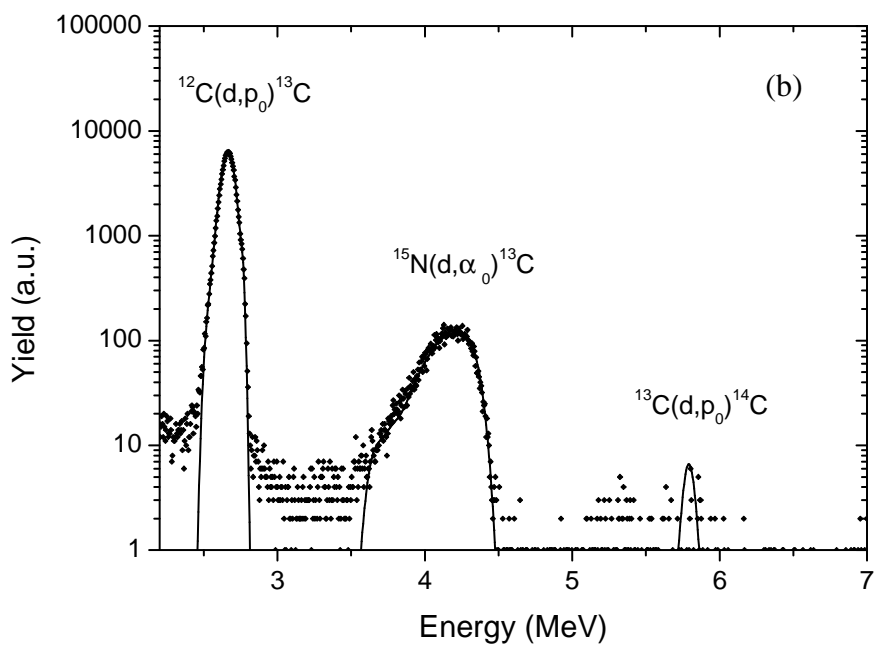
167 Figure 3: Depth distributions of ^{12}C (filled triangles) and ^{15}N (open squares) ions determined
168 from SIMNRA simulations for the copper sample implanted on the non deviated
169 beam line (2nd implantation).

170



171

172



173

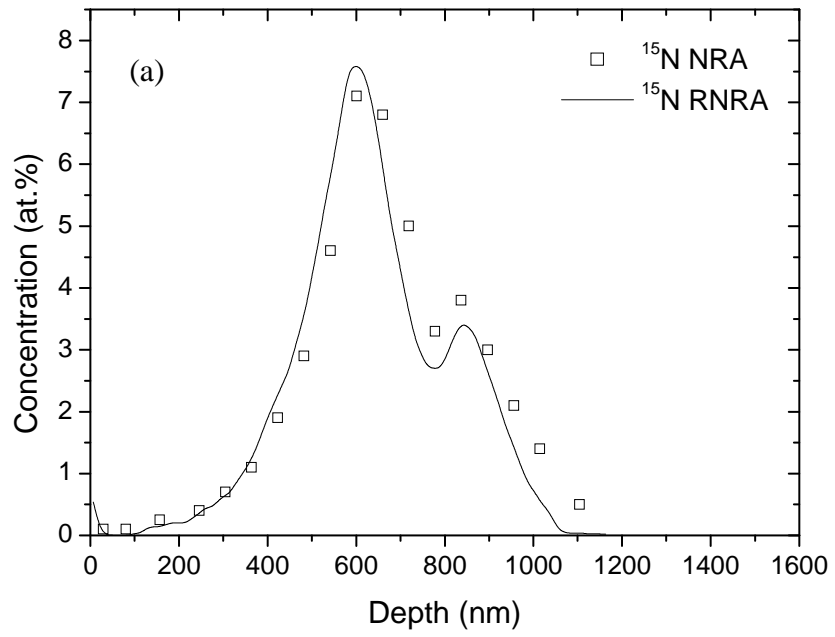
174

175

176

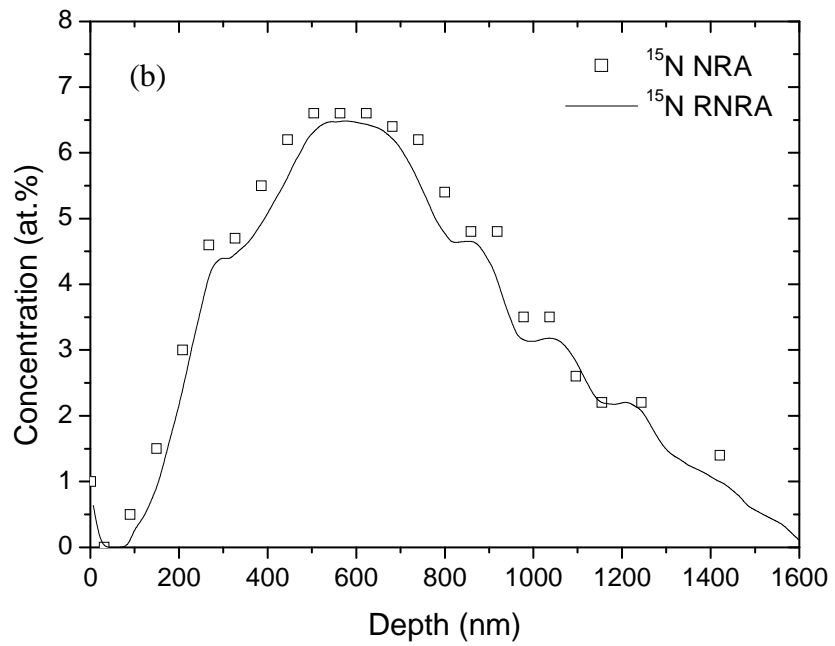
177

Figure 1



178

179



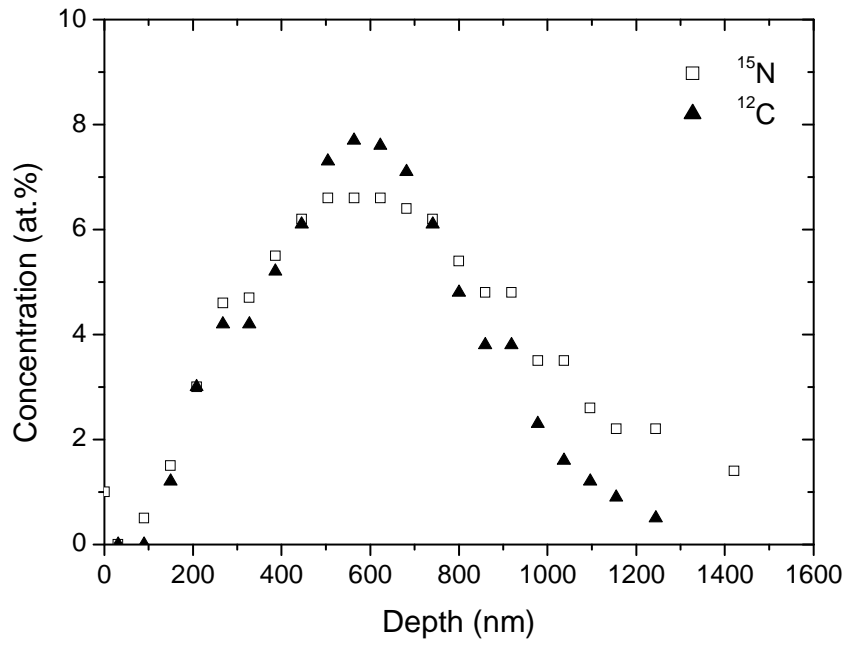
180

181

182

183

Figure 2



184
185
186
187

Figure 3